U.S. Department of the Interior
U.S. Geological Survey

Prepared for the
National Aeronautics and Space Administration

Scientific Investigations Map 3404
Sheet 2 of 2

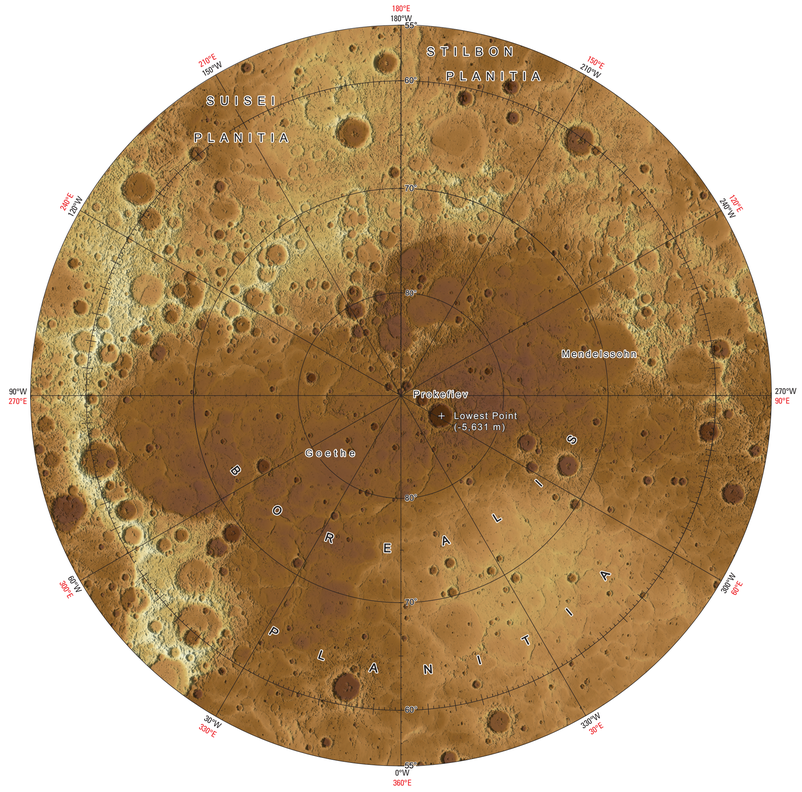

SCALE 1:12,157,366 (1 mm = 12.157366) AT 90° LATITUDE
POLAR STEREOGRAPHIC PROJECTION
West longitude (planetographic) coordinate system shown in black.
East longitude (planetocentric) coordinate system shown in red.

1000 500 0 500 1000 KILOMETERS
90 70 55

NORTH POLAR REGION

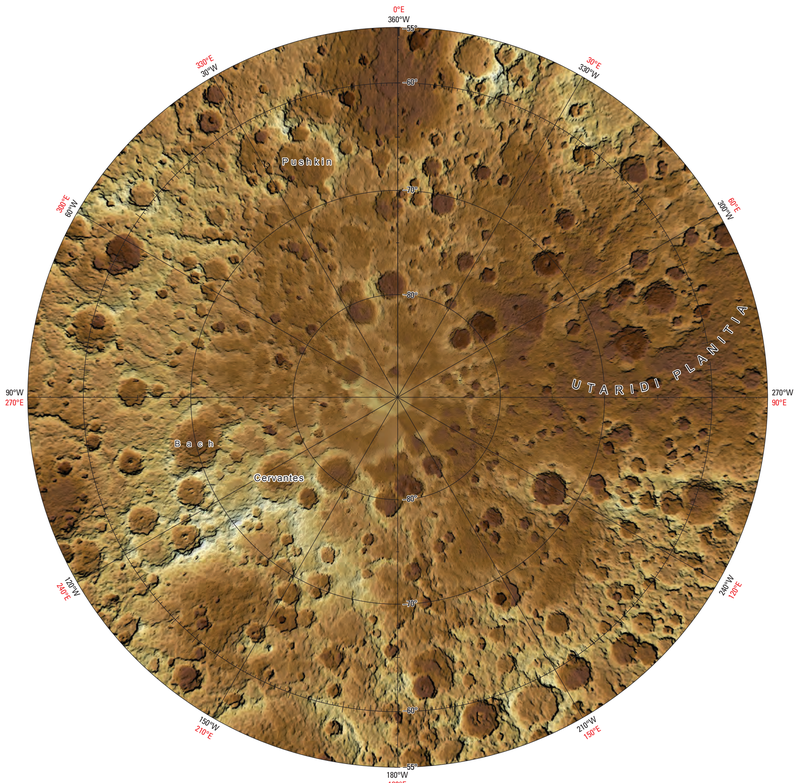

SCALE 1:12,157,366 (1 mm = 12.157366 km) AT –90° LATITUDE
POLAR STEREOGRAPHIC PROJECTION
West longitude (planetographic) coordinate system shown in black.
East longitude (planetocentric) coordinate system shown in red.

1000 500 0 500 1000 KILOMETERS
-90 -70 -55

SOUTH POLAR REGION

SPACECRAFT AND INSTRUMENT DESCRIPTION

This map is based on data acquired by the Mercury Dual Imaging System (MDIS; Hawkins and others, 2009) and Mercury Laser Altimeter (MLA; Cavanaugh and others, 2007) instruments on the National Aeronautics and Space Agency (NASA) MErcury Surface, Space ENvironment, GEochemistry, and Ranging (MESSENGER) spacecraft (Solomon and others, 2007). MDIS consists of two cameras, a wide angle camera (WAC) and a narrow angle camera (NAC). The WAC is a 4-element refractive telescope having a focal length of 78 millimeters (mm) and a collecting area of 48 mm^2. A 12-position filter wheel provides color imaging over the spectral range of the charge-coupled device (CCD) detector. Eleven spectral filters spanning the range from 395 nanometers (nm) to 1,040 nm are defined to cover wavelengths diagnostic of different surface materials. The twelfth position is a broad-band filter for optical navigation (Denevi and others, 2016). The NAC is an off-axis reflective telescope with a 550-mm focal length and a collecting area of 462 mm^2. The NAC has an identical CCD detector with a single medium-band filter (100 nm wide), centered at 750 nm to match to the corresponding WAC filter 7 (or G filter) for monochrome imaging (Hash and others, 2015). The MLA instrument uses a laser to measure the distance between the spacecraft and the surface. As a bi-static system (transmitter and receiver), the transmitter generates a brief laser pulse and the time is measured for the light to reach the surface and return into the receiver. This allows for accurate topographic measurements, with respect to Mercury's center of mass, even into completely shadowed regions (Sun and Neumann, 2015).

MAP DESCRIPTION

The topographic shaded-relief maps shown here were derived from two independently created digital elevation models (DEMs). The equatorial and south pole DEMs were generated from a sparse control network derived from MDIS WAC and NAC image-to-image feature-based matching (Becker and others, 2016). The north pole map was created by interpolating a DEM from dense MLA range measurements (fig. 1, Zuber and others, 2012).

Using the Integrated Software for Imagers and Spectrometers (ISIS3) image processing system (Sides and others, 2017) and 176,352 observations from MDIS NAC and wide-angle camera-G (WAC-G), a global DEM of Mercury was derived (Becker and others, 2016). The DEM was created with a least-squares bundle adjustment of common features, measured as tie-point coordinates in overlapping NAC and WAC-G filter images (Edmundson and others, 2012). Because the NAC and WAC-G observations were acquired with a large range of geometric and illumination characteristics, new methods were developed in ISIS3 to overcome these challenges. This new approach utilized unsupervised image-to-image feature-based matching and control techniques that are well suited for scaling and distribution across compute cluster environments (Becker and others, 2016).

From the 176,352 images, we selected a subset limited by pixel scale (75 to 800 meters per pixel; 64,986 NAC and 37,091 WAC-G images) and successfully controlled 100,432 images (63,536 NAC, 36,896 WAC-G) to sub-pixel accuracy (0.86 average pixel residual from the bundle adjustment). The final global control network contained 12,596,336 control points and 94,745,475 tie-point measurements. From this control network, a global DEM was interpolated at 64 pixels per degree (665 meters per pixel). During the interpolation step, for each DEM pixel, 11 points were selected and a 1.0-standard-deviation filter centered about the median radius was applied to eliminate outliers. The median radius was then selected from the remaining points as the output DEM radius value, and finally a series of averaging filters smoothed the final DEM (Becker and others, 2016). The lowest point of the MDIS-derived DEM occurs in the bottom of Rachmaninoff crater (crater at lat 27.66° N., long 302.63° W., and the highest point occurs at lat 8.73° S., long 241.24° W.).

MLA, primarily in the northern hemisphere, acquired more than 26 million measurements of Mercury's surface. The individual MLA footprints are ~80 meters (m) in diameter and on average are spaced ~350 to 450 m along track. The radial precision of individual measurements is <1 m, and the accuracy with respect to Mercury's center of mass is better than 20 m (Zuber and others, 2012). From these topographic measurements, despite larger coverage gaps poleward of lat 84° N., a high-precision DEM was created using a spline tension interpolation within the Generic Mapping Tool suite at 500 meters per pixel. In contrast to the MDIS-derived DEM, the lowest point in the MLA-derived DEM is found in Prokofiev crater (lat 85.46° N., long 296.21° W.). The MLA data does confirm the general location for the MDIS-derived highest point, although a prominent portion of the Raditladi crater rim (lat 30.36° N., long 243.19° W.) may exceed the MDIS-derived height (G.A. Neumann, NASA Goddard Space Flight Center, written commun., 2018). Precise global laser altimetric coverage awaits completion by future missions.

PROJECTION

The Mercator projection is used between latitudes ±57°, with a central meridian at 0° longitude and latitude equal to the nominal scale at 0°. The polar stereographic projection is used for the regions north of the +55° parallel and south of the –55° parallel, with a central meridian set for both at 0° and a latitude of true scale at +90° and –90°, respectively. The adopted spherical radius used to define the map scale is 2439.4 km (Perry and others, 2015).

COORDINATE SYSTEM

The orientation model for Mercury has been updated using improved pole position and short-period longitude libration data from Margot (2009). The International Astronomical Union (IAU) Working Group, since its original report (Davies and others, 1980), continues to recommend the use of the crater Hun Kal (which means "twenty" in the Mayan language) to define the 20° west longitude meridian. Therefore, the value of the prime meridian (W0) used previously (W0 = 329.548°; Robinson and others, 1999) but corrected for libration terms at J2000.0 results in a new recommended value of W0 = 329.5988° (Stark, 2016).

Longitudes are shown in both positive West (shown in black) and East (shown in red). Positive West is the default longitude system recommended by the IAU (Archinal and others, 2011), but positive East has been used for all MESSENGER map products.

MAPPING TECHNIQUES

The topographic shaded-relief maps were generated from the original MDIS- and MLA-based DEMs with a sun angle of 45° from horizontal and a Sun azimuth of 270°, as measured clockwise from north, with no vertical exaggeration. The DEM values were then mapped to a global color look-up table, with each color representing a range of 1 km of elevation. The shaded-relief and color files were then merged and scaled to 1:20,000,000 for the Mercator portion and 1:12,157,366 for the two polar stereographic parts with a resolution of 300 pixels per inch. The two projections have a common scale at ±56° latitude.

NOMENCLATURE

Feature names on this sheet have been approved by the IAU. All features greater than 200 km in diameter or length were included unless they were not visible at the printed map scale. Some selected well-known features less than 200 km in diameter or length were also included. For a complete list of the IAU-approved nomenclature for Mercury, see the Gazetteer of Planetary Nomenclature at https://planetarynames.wr.usgs.gov.

ACKNOWLEDGMENTS

The collection of data used in the production of this map was made possible by NASA, the MESSENGER mission, and the Mercury Digital Imaging System and Mercury Laser Altimeter teams. Costs of map production and publication were funded by a NASA and U.S. Geological Survey Interagency Agreement.

REFERENCES CITED

Acton, C.H., 1996, Ancillary Data Services of NASA's Navigation and Ancillary Information Facility: Planetary and Space Science, v. 44, no. 1, p. 65–70, https://naif.jpl.nasa.gov/naif/.

Archinal, B.A. (chair), A'Hearn, M.F., Bowell, E., Conrad, A., Consolmagno, G.J., Courtin, R., Fukushima, T., Hestroffer, D., Hilton, J.L., Krasinsky, G.A., Neumann, G., Oberst, J., Seidelmann, P.K., Stooke, P., Tholen, D.J., Thomas, P.C., and Williams, I.P., 2011, Report of the IAU Working Group on Cartographic Coordinates and Rotational Elements—2009: Celestial Mechanics and Dynamical Astronomy, v. 109, no. 2, p. 101–135, https://doi.org/10.1007/s10569-010-9320-4.

Becker, K.J., Robinson, M.S., Becker, T.L., Weller, L.A., Edmundson, L., Neumann, G.A., Perry, M.E., and Solomon, S.C., 2016, First global digital elevation model of Mercury, *in* Lunar and Planetary Science Conference, XLVII: The Woodlands, Tex., Lunar and Planetary Institute, abstract no. 2959.

Cavanaugh, J.F., Smith, J.C., Sun, X, Bartels, A.E., Ramos-Izquierdo, L., Krebs, D.J., Novo-Gradac, A.M., McGarry, J.F., Trunzo, R., Britt, J.L., Karsh, J., Katz, R.B., Lukemire, A., Szymkiewicz, R., Berry, D.L., Swinski, J.P., Neumann, G.A., Zuber, M.T., and Smith, D.E., 2007, The Mercury Laser Altimeter instrument for the MESSENGER mission: Space Science Reviews, v. 131, p. 451–479.

Davies, M.E., Abalakin, V.K., Cross, C.A., Duncombe, R.L., Masursky, H., Morando, B., Owen, T.C., Seidelmann, P.K., Sinclair, A.T., Wilkins, G.A., and Tjuflin, Y.S., 1980, Report of the IAU Working Group on Cartographic Coordinates and Rotational Elements of the Planets and Satellites: Celestial Mechanics and Dynamical Astronomy, v. 22, p. 205–230.

Denevi, B.W., Seelos, F.P., Ernst, C.M., Keller, M.R., Chabot, N.L., Murchie, S.L., Domingue, D.L., Hash, C.D., and Blewett, D.T., 2016, Final calibration and multispectral map products from the Mercury Dual Imaging System wide-angle camera on MESSENGER, *in* Lunar and Planetary Science Conference, XLVII: The Woodlands, Tex., Lunar and Planetary Institute, abstract no. 1264, https://www.hou.usra.edu/meetings/lpsc2016/pdf/1264.pdf.

Edmundson, K.L., Cook, D.A., Thomas, O.H., Archinal, B.A., and Kirk, R.L., 2012, Jigsaw—The ISIS3 bundle adjustment for extraterrestrial photogrammetry: International Society for Photogrammetry and Remote Sensing Annals of Photogrammetry, Remote Sensing, and Spatial Information Sciences, v. I-4, p. 203–208.

Hash, C., Espiritu, R., Malaret, E., Prockter, L., Murchie, S., Mick, A., and Ward, J., 2015, MESSENGER Mercury Dual Imaging System (MDIS) Experiment Data Record (EDR) Software Interface Specification (SIS): The Johns Hopkins University, Applied Physics Laboratory, MDIS EDR SIS V2T, https://pdsimage2.wr.usgs.gov/archive/mess-e_v_h-mdis-2-edr-rawdata-v1.0/MSGRMDS_1001/DOCUMENT/MDISEDRSIS.PDF.

Hawkins, S.E., III, Murchie, S.L., Becker, K.J., Selby, C.M., Turner, F.S., Nobel, M.W., Chabot, N.L., Choo, T.H., Darlington, E.H., Denevi, B.W., Domingue, D.L., Ernst, C.M., Holsclaw, G.M., Laslo, N.R., McClintock, W.E., Prockter, L.M., Robinson, M.S., Solomon, S.C., and Sterner, R.E., II, 2009, In-flight performance of MESSENGER's Mercury Dual Imaging System, *in* Hoover, B., Levin, G.V., Rozanov, A.Y., and Retherford, K.D., eds., Instruments and methods for Astrobiology and Planetary Missions XII: Bellingham, Wash., SPIE, Proceedings 7441, Paper 74410Z, 12 p.

Margot, J.L., 2009, A Mercury orientation model including non-zero obliquity and librations: Celestial Mechanics and Dynamical Astronomy, v. 105, no. 4, p. 329–336, https://doi.org/10.1007/s10569-009-9234-1.

Perry, M.E., Neumann, G.A., Phillips, R.J., Barnouin, O.S., Ernst, C.M., Kahan, D.S., Solomon, C., Zuber, M.T., Smith, D.E., Hauck, S.A., II, Peale, S.J., Margot, J., Mazarico, E., Johnson, C.L., Gaskell, R.W., Roberts, J.H., McNutt, R.L., Jr., and Oberst, J., 2015, The low-degree shape of Mercury: Geophysical Research Letters, v. 42, p. 6951–6958, https://doi.org/10.1002/2015GL065101.

Robinson, M.S., Davies, M.E., Colvin, T.R., and Edwards, K., 1999, A revised control network for Mercury: Journal of Geophysical Research, v. 104, no. E12, p. 30847–30852.

Sides, S.C., Becker, T.L., Becker, K.J., Edmundson, K.L., Backer, J.W., Wilson, T.J., Weller, L.A., Humphrey, I.R., Berry, K.L, Shepherd, M.R., Hahn, M.A., Rose, C.C, Rodriguez, R., Paquette, A.C., Mapel, J.A., Shinaman, J.R., and Richie, J.O., 2017, USGS Integrated Software for Imagers and Spectrometers (ISIS3) instrument support, new capabilities, and releases *in* Lunar and Planetary Science Conference, XLVIII: The Woodlands, Tex., Lunar and Planetary Institute, abstract no. 2739.

Solomon, S.C., McNutt Jr., R.L., Gold, R.E., and Domingue, D.L., 2007, MESSENGER mission overview: Space Science Reviews, v. 131, p. 3–39, https://doi.org/10.1007/s11214-007-9247-6.

Stark, A., 2016, The prime meridian of the planet Mercury: unpublished report available at ftp://naif.jpl.nasa.gov/pub/naif/pds/data/mess-e_v_h-spice-6-v1.0/messsp_1000/document/stark_prime_meridian.pdf.

Sun, X., and Neumann, G.A., 2015, Calibration of the Mercury Laser Altimeter on the MESSENGER Spacecraft: IEEE Transactions on Geoscience and Remote Sensing, v. 53, no. 5, p. 2860–2874.

Zuber, M.T., Smith, D.E., Phillips, R.J., Solomon, S.C., Neumann, G.A., Hauck, S.A., Peale, S.J., Barnouin, O.S., Head, J.W., Johnson, C.L., Lemoine, F.G., Mazarico, E., Sun, X., Torrence, M.H., Freed, A.M., Klimczak, C., Margot, J., Oberst, J., Perry, M.E., McNutt, R.L., Balcerski, J.A., Michel, N., Talpe, M.J., and Yang, D., 2012, Topography of the northern hemisphere of Mercury from MESSENGER laser altimetry: Science, p. 217–220, https://doi.org/10.1126/science.1218805.

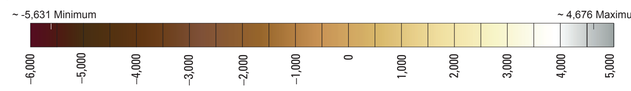

ELEVATION IN METERS

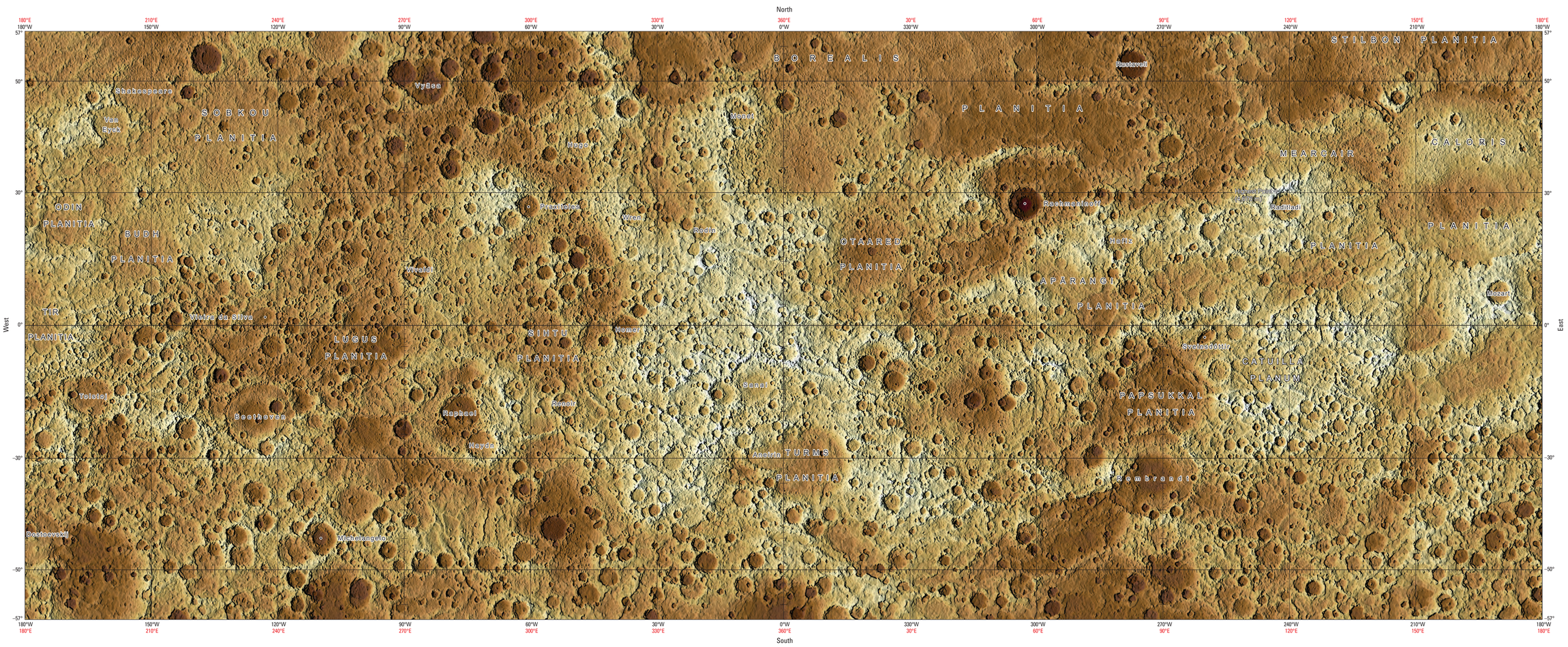

SCALE 1:20,000,000 (1 mm = 20 km) AT 0° LATITUDE
MERCATOR PROJECTION
West longitude (planetographic) coordinate system shown in black.
East longitude (planetocentric) coordinate system shown in red.

2000 1000 500 0 500 1000 2000 KILOMETERS
57 40 20 0

Descriptions of nomenclature used on map are listed at https://planetarynames.wr.usgs.gov

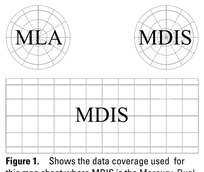

Figure 1. Shows the data coverage used for this map sheet where MDIS is the Mercury Dual Imaging System and MLA is the Mercury Laser Altimeter.

Topographic Map of Mercury

By

Marc A. Hunter,[1] Trent M. Hare,[1] Rosalyn K. Hayward,[1] Kris J. Becker,[2] Tammy L. Becker,[1] Lynn A. Weller,[1] Kenneth L. Edmundson,[1] Gregory A. Neuman,[3] Erwan Mazarico,[3] Mark E. Perry,[4] and Sean C. Solomon[5]

2018

[1]U.S. Geological Survey,
[2]University of Arizona,
[3]NASA Goddard Space Flight Center,
[4]Johns Hopkins University,
[5]Columbia University

Prepared on behalf of the Planetary Science Division, Science Mission Directorate, National Aeronautics and Space Administration

Edited by J.L. Zigler; digital cartography by D.L. Knifong and Katie Sullivan

Manuscript approved for publication April 2, 2018

ISSN 2329-1311 (print)
ISSN 2329-132X (online)
https://doi.org/10.3133/sim3404

For sale by U.S. Geological Survey, Information Services, Box 25286, Federal Center, Denver, CO 80225, 1–888–ASK–USGS

Digital files available at https://doi.org/10.3133/sim3404

Suggested citation: Hunter, M.A., Hare, T.M., Hayward, R.K., Chabot, N.L., Hash, C.D., Denevi, B.W., Ernst, C.M., Murchie, S.L., Blewett, D.T., Malaret, E.R., Solomon, S.C., Becker, K.J., Becker, T.L., Weller, L.A., Edmundson, K.L., Neuman, G.A., Mazarico, E., and Perry, M.E., 2018, Image mosaic and topographic maps of Mercury: U.S. Geological Survey Scientific Investigations Map 3404, scale 1:20,000,000 and 1:12,157,366, https://doi.org/10.3133/sim3404.